ISSN 0965-5441, Petroleum Chemistry, 2021, Vol. 61, No. 7, pp. 739–747. © Pleiades Publishing, Ltd., 2021.
Russian Text © The Author(s), 2021, published in Neftekhimiya, 2021, Vol. 61, No. 4, pp. 494–503.

Hydroconversion of *n*-Hexadecane on Zeolite-Containing Sulfide-Based Catalysts: Influence of Nitrogen Impurity in the Feedstock on the Hydroisomerization Selectivity

N. A. Vinogradov[a], M. I. Rubtsova[b], A. P. Glotov[b], N. V. Tochilin[a], V. A. Vinokurov[b], and A. A. Pimerzin[a,b,c,*]

[a] *Samara State Technical University, Samara, 443100 Russia*
[b] *Gubkin Russian State University of Oil and Gas, Moscow, 119991 Russia*
[c] *LLC Gazpromneft-Industrial Innovations, St. Petersburg, 197350 Russia*
**e-mail: al.pimerzin@gmail.com*

Received February 10, 2021; revised April 7, 2021; accepted June 1, 2021

Abstract—Bifunctional zeolite-containing catalysts based on transition metal sulfides were synthesized, their physicochemical characteristics were determined, and the catalytic properties toward *n*-hexadecane hydroconversion were examined. ZSM-5, Beta, and NH_4NaY zeolites were tested as acidic components of the catalysts. The highest selectivity toward isomerization reaction was afforded by the NH_4NaY zeolite-containing sulfide-based catalyst. With the view to controlling the selectivity toward cracking and isomerization reactions, the influence of the presence of nitrogen-containing bases in the feedstock was evaluated.

Keywords: bifunctional catalysts, sulfide-based catalysts, composite supports, linear alkanes, hydroconversion, zeolites

DOI: 10.1134/S0965544121070057

Reactions of hydroconversion of linear alkanes underlie the most important processes used in petrochemical industry and petroleum refinery. For example, hydroisomerization of *n*-alkanes of light gasoline fractions into their corresponding branched forms is conducive to improvement of octane number of straight-run gasolines, as well as of low-temperature performance of diesel fuels and hydrocarbon base oils of lubricants [1–3].

In recent years, diesel fuel consumption has been increasing steadily, especially in cold climates [4]. Production of fuels with improved low-temperature performance relies on several technical practices and catalytic processes. One of the most common practices consists in increasing the fractional composition content of lighter components. This prevents high-molecular-weight hydrocarbons from getting into marketable fuels but at the same time causes depletion of the raw materials base of production. From this perspective, use of catalytic processes seems more attractive. Selective hydrocracking results in long-chain *n*-alkane splitting into two smaller molecules, leading to reduction in the cloud point and pour point [5]. Hydroisomerization allows improving the low-temperature characteristics of the feedstock via skeletal isomerization of long-chain alkanes with formation of branched isomers [6]. In both cases catalytic hydroconversion enables reducing the content of *n*-paraffinic hydrocarbons in the feedstock [7, 8]. Apart from that, the hydroisomerization route allows maintaining higher yields of diesel fuel with improved low-temperature characteristics and minimizing the yield of gaseous hydrocarbons.

Catalysts used in industrial hydrodewaxing and hydroisomerization processes typically comprise expensive platinum group metals (hydrogenating components) and silicoaluminophosphates (acidic components) [9–11]. However, noble metal-based catalysts have extremely poor resistance to catalytic

poisons, in particular, low sulfur tolerance [12]. Accordingly, considerable research efforts are being directed now at development of noble metal-free catalysts more tolerant to poisoning. For example, widely used components of hydrotreating catalysts are transition metal sulfides which afford sufficient catalytic activity in hydrogenation/dehydrogenation reactions while comparing favorably with noble metals in terms of their cost [13–15].

Different types of zeolites, zirconium oxides, natural clays, and mesoporous aluminosilicates find use as acidic components of bifunctional catalysts [16–18]. The best performance in hydroisomerization reactions is exhibited by SAPO-11 silicoaluminophosphates [19]. However, in some cases the cracking function of the catalyst is useful alongside the isomerization function. This applies, e.g., to the case of adjusting the fractional composition content of the hydrogenation product while increasing the gasoline yield from heavy feedstock [20, 21]. Various approaches were tested for tuning the selectivity of hydroconversion process, e.g., via changing the number of hydrogenating active sites [22], the type of the hydrogenation component [23], and the type/amount of acid component, specifically zeolite [24–27]. Use of zeolite-containing transition metal sulfide-based catalysts typically results in the dominance of cracking reactions [28, 29].

Some studies demonstrated the predominant deactivation of bifunctional noble metal-based catalysts in the cracking reactions run in the presence of nitrogen-containing compounds in the feedstock [12, 30, 31]. This suggests that processing of nitrogen-containing feedstock or use of nitrogen-containing additives to the prepared feedstock may provide a means for tuning the selectivity of the hydroconversion process. Insufficiently studied for bifunctional transition metal sulfide-based catalysts, this approach is of both scientific and industrial importance.

Herein, we report on the synthesis and study of catalysts based on comparatively less expensive sulfides and ZSM-5, Beta, and Y zeolites as applied to *n*-hexadecane hydroconversion reaction with the view to assessing the prospects for tuning the process selectivity by adding nitrogen-containing compounds to the feedstock.

EXPERIMENTAL

Samples of routinely used commercial zeolites NH_4NaY (Si/Al = 2.5), Beta (Si/Al = 30), and ZSM-5 (Si/Al = 30) served as acidic additives. Composite catalyst supports were produced as extrudate granules with a diameter of 1 mm and a length of 2 mm using pseudoboehmite (Sasol Company, Germany) as a binder and nitric acid as a peptizing agent. The extrudates were dried at 80–120°C for 6 h and then calcined at 550°C for 4 h. After calcination the composite support contained 40 wt % NH_4NaY, Beta, or ZSM-5 and 60 wt % γ-Al_2O_3.

CoMo catalysts were prepared by single-dip incipient wetness impregnation of the support with the solution of active component precursors: phosphomolybdic acid ($H_3PMo_{12}O_{40}\cdot 18H_2O$), cobalt carbonate hydroxide hydrate [$CoCO_3\cdot mCo(OH)_2\cdot nH_2O$], and chemically pure citric acid. For the synthetic procedure, see [32]. After impregnation the samples were dried at 60°C for 2 h, at 80°C for 2 h, and at 110°C for 6 h. The estimated content of molybdenum(VI) oxide in the catalysts was 15 wt %, and that of cobalt(II) oxide, 3.5 wt %. The active metal loadings were chosen based on the published data and on our own research results [14, 33, 34]. The content of the metals in the catalysts synthesized was monitored using an EDX-800HS Shimadzu X-ray fluorescence analyzer.

The textural characteristics of the composite supports were determined by low-temperature nitrogen adsorption on a Quantachrome Autosorb-1 surface area and pore size analyzer. The specific surface area was calculated using the Brunauer–Emmett–Teller (BET) model in the relative pressure range p/p_0 = 0.05–0.3. The total pore volume and pore size distribution were determined from the desorption branch of the isotherm using the Barrett–Joyner–Halenda model. The micropore characteristics were evaluated by the t-plot method.

For analyzing the acidic properties of the materials was used the method of temperature-programmed desorption of ammonia (NH_3–TPD). The experiments consisted of three stages. In the first (preparation) stage the adsorbed water was removed from the pores at a temperature of 120°C in a helium flow for 5 h (heating rate 10°C min^{-1}). The second stage involved ammonia adsorption from a mixture of 10 vol % NH_3 in helium (gas flow rate 30 cm^3 min^{-1}) at a temperature of 60°C (heating rate 10°C min^{-1}) for 30 min, whereupon the unbound NH_3 was removed at a temperature of 60°C in a helium flow for 60 min. In the third stage, NH_3 was desorbed in a helium flow with heating to 750°C (heating rate 8°C min^{-1}) and holding at this temperature for 45 min.

The catalytic properties of the bifunctional catalysts were examined in a laboratory fixed-bed flow reactor. A 1.5 cm^3 volume of the catalyst (0.25–0.50 mm particles)

Table 1. Results of the catalytic tests for hydroconversion of *n*-hexadecane[a]

Catalyst	Conversion	280°C	300°C	320°C
$CoMo/Al_2O_3$–Beta(40%)	X_{iso}	<3	<3	<3
	X_{cr}	>95	>95	>95
$CoMo/Al_2O_3$–ZSM-5(40%)	X_{iso}	3	3	3
	X_{cr}	>95	>95	>95
$CoMo/Al_2O_3$–ZSM-5(5%)	X_{iso}	<3	3	3
	X_{cr}	30	66	>95
$CoMo/Al_2O_3$–NH_4NaY(40%)	X_{iso}	<3	5	9
	X_{cr}	10	19	27

[a] At 1.5 MPa H_2, WHSV 1 h^{-1}, and H_2/feedstock volumetric ratio 150 nL/L.

was loaded into the isothermal region of the reactor. Gas phase sulfidation of the CoMo catalysts was carried out at 400°C and 1 MPa in a H_2S/H_2 flow (10/90 vol %) for 4 h. As a model feedstock for evaluating the catalyst performance in hydroisomerization reaction was used a mixture of *n*-hexadecane (3 wt %) in *n*-heptane as a solvent. Under noncatalytic treatment conditions the selected substrates were not subjected to chemical transformations. The catalytic activity was analyzed under the following conditions: temperature range 280–360°C, 1.5 MPa H_2, weight hourly space velocity (WHSV) 1–3 h^{-1}, and volume ratio of H_2 to feedstock 150 nL/L.

Product identification was performed on a gas chromatograph with a Shimadzu GCMS-QP2010 quadrupole mass detector equipped with a flame ionization detector and a 30 m × 0.5 mm × 0.5 μm column (OV-101 nonpolar phase, dimethylpolysiloxane as stationary phase). Analysis conditions: detector temperature 250°C, vaporizer temperature 250°C; temperature program: isothermal for 2 min at 110°C, then heating to 250°C at 5°C/min. Flow rate of the carrier gas (helium) was 3 mL/min, and velocity, 30 cm/s. For achieving conversion in a steady state, the hydroconversion process was run for at least 8 h under constant reaction conditions.

The products were identified on a Shimadzu single quadrupole GCMS-QP2010 gas chromatograph-mass detector equipped with a 100 m × 0.25 mm × 0.5 μm nonpolar Agilent DB-Petro column (dimethylpolysiloxane as stationary phase). Analysis conditions: vaporizer temperature 250°C, detector temperature 200°C; temperature program: isothermal for 10 min at 140°C, then heating to 290°C at 5°C/min, then holding isothermally at 290°C for 20 min. The carrier gas (helium) flow rate was 3 mL min^{-1}, and linear velocity, 30 cm/s.

The conversion and isomerization selectivity were calculated using the following equations:

$$X_{iso} = \frac{iso\text{-hexadecanes}}{\text{initial}\, n\text{-hexadecane}},$$

$$Sel_{iso} = \frac{iso\text{-hexadecanes}}{\text{consumed}\, n\text{-hexadecane}}.$$

The reaction rate constant for hydroisomerization was determined by the equation:

$$k_{iso} = -\frac{F}{m}\ln(1 - X_{iso}),$$

where k_{iso} is the pseudo-first-order reaction constant for *n*-hexadecane hydroisomerization, mol g^{-1} h^{-1}; X_{iso}, *n*-hexadecane conversion, %, to C_{16} isomers; *F*, reactant (*n*-hexadecane) flow, mol/h, and *m*, weight of the catalyst, g.

RESULTS AND DISCUSSION

Table 1 presents the results of the catalytic tests. The catalysts containing Beta and ZSM-5 zeolites as acidic additives showed high cracking activity, while isomerization products were almost completely absent. Throughout the 280–320°C temperature range examined the hexadecane cracking efficiency exceeded 95%. Hence, the catalysts tested in this study can find application in heavy feedstock processing with the aim of obtaining incremental yields of light components in commercial products.

For inhibition the cracking reactions and increasing the selectivity of the isomerization process we prepared $CoMo/Al_2O_3$–ZSM-5(5%) catalyst with a lower content (5 wt %) of acidic additive (ZSM-5), since acid sites of the catalyst are specifically responsible for cracking reactions. However, a decrease in the ZSM-5 content

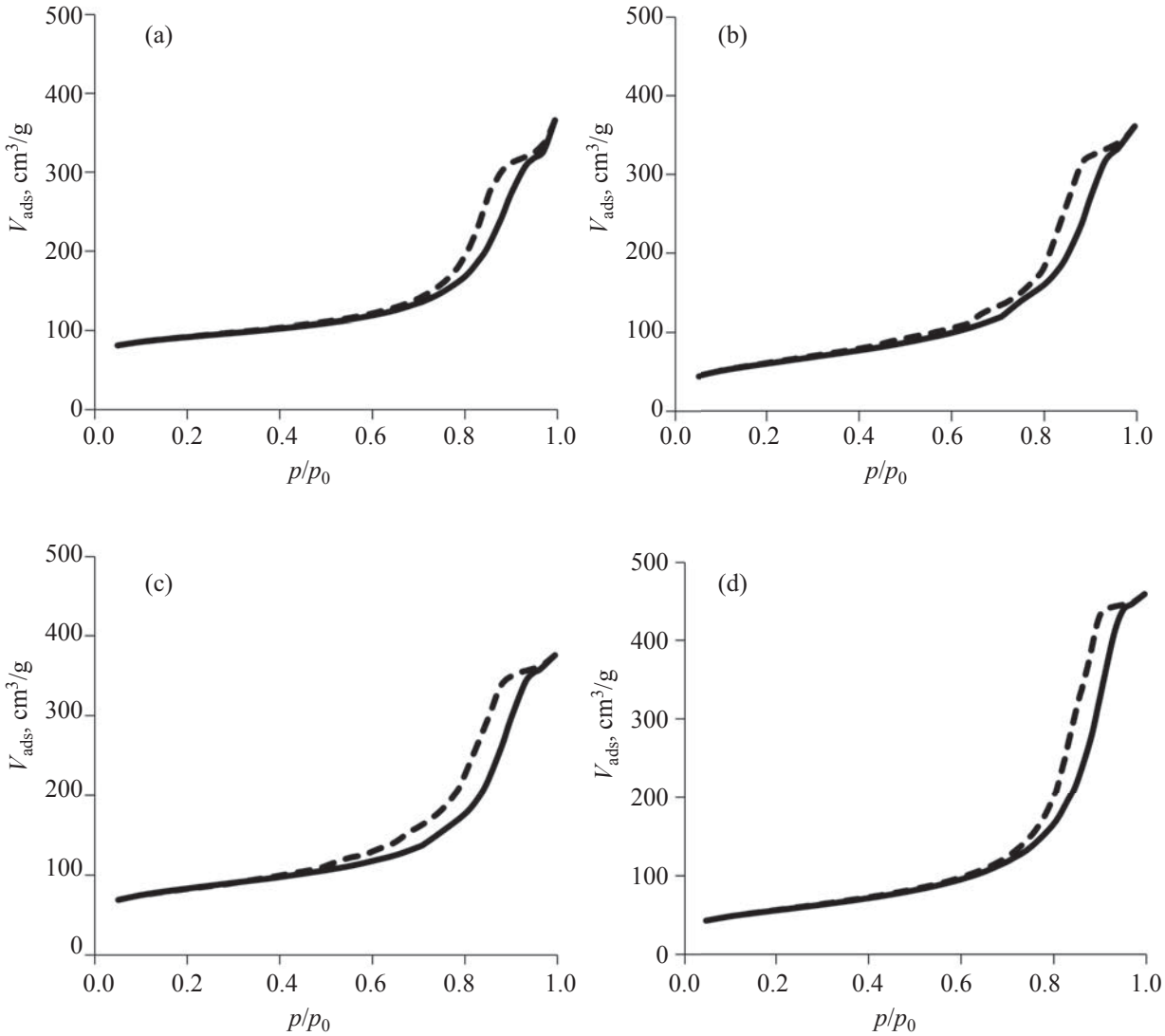

Fig. 1. Nitrogen adsorption–desorption isotherms at 77 K for the supports: (a) Al_2O_3–NH_4NaY(40%), (b) Al_2O_3–Beta(40%), (c) Al_2O_3–ZSM-5(40%), and (d) Al_2O_3–ZSM-5(5%).

in the catalyst did not cause any noticeable increase in selectivity of isomerization. The cracking route prevailed in the hydroconversion of *n*-hexadecane over CoMo/Al_2O_3–ZSM-5(5%) catalyst. A sufficiently high selectivity of isomerization at moderate cracking activity was achieved only with the use of the NH_4NaY zeolite-based catalyst. While exhibiting lower overall activity, this catalyst provided a close to 10% isomerization efficiency at 320°C at the cracking efficiency not exceeding 30%. The differences in the catalytic properties between the catalysts tested are directly related to their physicochemical properties.

Figure 1 shows the low-temperature nitrogen adsorption–desorption isotherms of the composite supports synthesized. These are Type IV isotherms which are typical of mesoporous materials. H3-type hysteresis loops are indicative of slit-like pores characteristic of mesoporous alumina [35]. Table 2 describes the textural properties of the samples obtained. All the samples were characterized by the same mesopore size of ~12 nm, usually exhibited by alumina produced from pseudoboehmite, which suggests reproducibility of the preparation conditions. The micropore areas and volumes determined for the samples containing 40 wt % zeolite additive corresponded to the textural characteristics

Table 2. Textural characteristics of the catalyst supports and zeolite additives

Sample	S_{BET}, m^2/g	V_{pore}, cm^3/g	D, nm	S_{micro}, m^2/g	V_{micro}, m^2/g
Al_2O_3–NH_4NaY(40%)	293	0.489	12	143	0.073
Al_2O_3–Beta(40%)	282	0.525	12	109	0.057
Al_2O_3–ZSM-5(40%)	276	0.542	12	92	0.046
Al_2O_3–ZSM-5(5%)	195	0.728	12	–	–
NH_4NaY	703	0.357	–	690	0.360
Beta	483	0.315	–	380	0.198
ZSM-5	253	0.156	–	236	0.122

Table 3. Acidic properties of the supports synthesized

Sample	Acidity according to the NH_3–TPD data, μmol/g			
	LT[a]	MT[a]	HT[a]	total
Al_2O_3–NH_4NaY(40%)	589	370	353	1312
Al_2O_3–Beta(40%)	544	360	372	1276
Al_2O_3–ZSM-5(40%)	490	495	250	1235
Al_2O_3–ZSM-5(5%)	254	361	440	1055

[a] (LT) Low-temperature (100–300°C), (MT) medium-temperature (300–600°C), and (HT) high-temperature (600–750°C) acidic active sites.

of the original zeolites, also presented in Table 2. The largest specific surface area and micropore volume were exhibited by the NH_4NaY zeolite-containing sample. The textural characteristics of the Al_2O_3–ZSM-5(5%) sample were most similar to those of conventional mesoporous γ-Al_2O_3, which finding can be explained by a low content of the additive and limitations of the t-plot method [36]. Overall, no significant differences in the textural properties between the supports synthesized were revealed.

Figure 2 demonstrates the NH_3–TPD curves for the supports tested. All the curves exhibited three distinct segments with maxima near 220, 450, and 700°C, corresponding to acid sites of different strengths. Quantitatively evaluation of the acidic properties of the samples synthesized (see Table 3) revealed close total acidities for all the supports, except for the sample added with the smallest zeolite amount, as reasonably expected. The samples containing zeolite ZSM-5 were characterized by a large number of medium-temperature acidic sites.

High cracking activity exhibited by the Beta- and ZSM-5 zeolite-containing catalysts may be attributed to high acidity of the zeolites and to small size of micropores, which caused diffusion limitations, thereby extending the contact time between the substrate molecules and the acidic active sites within the crystals [10, 37, 38]. A decrease in the amount of the zeolite added did not cause major increase in selectivity toward isomerization reaction, since the number of the medium-temperature acidic active sites enhancing the cracking reactions decreased insignificantly. The decrease in the total acidity of the support added with a smaller zeolite amount was not proportional to the amount of the additive. This may be due to a more efficient distribution of a small amount

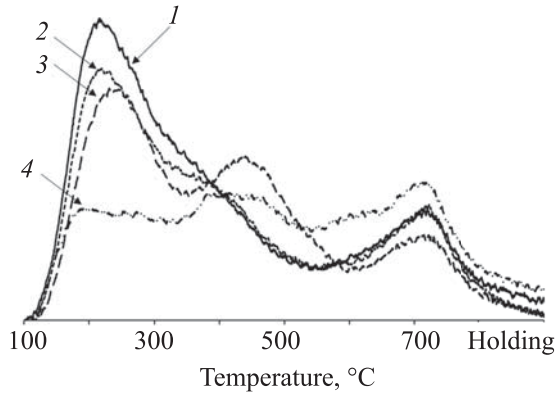

Fig. 2. NH_3–TPD curves for the supports: (*1*) Al_2O_3–NH_4NaY(40%), (*2*) Al_2O_3–Beta(40%), (*3*) Al_2O_3–ZSM-5(40%), and (*4*) Al_2O_3–ZSM-5(5%).

Table 4. Results of testing the NH_4NaY zeolite-containing catalyst for hydroconversion of the feedstock in the presence of nitrogen-containing compounds[a]

Temperature, °C	320	340	360	340	360	360
Nitrogen content in feedstock, ppm	–	–	–	50	50	150
Conversion, %, in indicated reaction:						
– isomerization	9	13	18	8	11	5
– cracking	27	37	44	4	9	5
Sel_{iso}, %	19	26	29	67	55	50

[a] At 1.5 MPa H_2, WHSV 1 h^{-1}, and H_2/feedstock volumetric ratio 150 nL/L.

of the zeolite additive, affording additional acid sites via zeolite-binder interaction [39, 40].

Relatively high selectivity toward isomerization reaction at moderate cracking activity achieved with the NH_4NaY zeolite-containing catalyst (Table 4) may be due to its moderate acidity represented by equal amounts of Lewis and Brønsted acid sites, which favors the hydroisomerization reaction [41, 42]. Linear first-order reaction equation fits well our experimental results (Fig. 3). The observed rate constant of the isomerization reaction on the NH_4NaY zeolite-based catalyst was estimated at 4.74×10^5 mol g^{-1} h^{-1} at 360°C, with 30% selectivity of the reaction toward isomers.

With the view to improving the selectivity of *n*-hexadecane hydroisomerization in the presence of the NH_4NaY-containing catalyst synthesized, we evaluated how it was influenced by the presence of nitrogen-containing compounds in the feedstock. Quinoline in amounts providing 50 and 150 ppm nitrogen concentration in the feedstock served as a nitrogen source. It is worth mentioning that quinoline was not detected among the hydrogenation products. Adding 50 ppm nitrogen to the feedstock caused reduction of the rate of the cracking reactions by nearly an order of magnitude, from 1.12×10^4 to 1.57×10^5 mol g^{-1} h^{-1} at 360°C (Fig. 4). This was due to predominant adsorption of quinoline on strong acid sites under the experimental conditions, which promoted the cracking reaction [43]. The resultant deceleration of the hydroisomerization reaction led to an almost threefold (from 23 to 61%) increase in selectivity toward isomerization. The beneficial effect produced by the inhibition is attributable to the fact that suppression of a part of the acid sites led to a balance between the acid sites and the hydrogenation sites that is optimal for the hydroisomerization reaction [44]. An increase in the nitrogen content in the feedstock to 150 ppm significantly inhibited the isomerization reaction as well, because nitrogen-containing bases were also adsorbed on weaker acid sites.

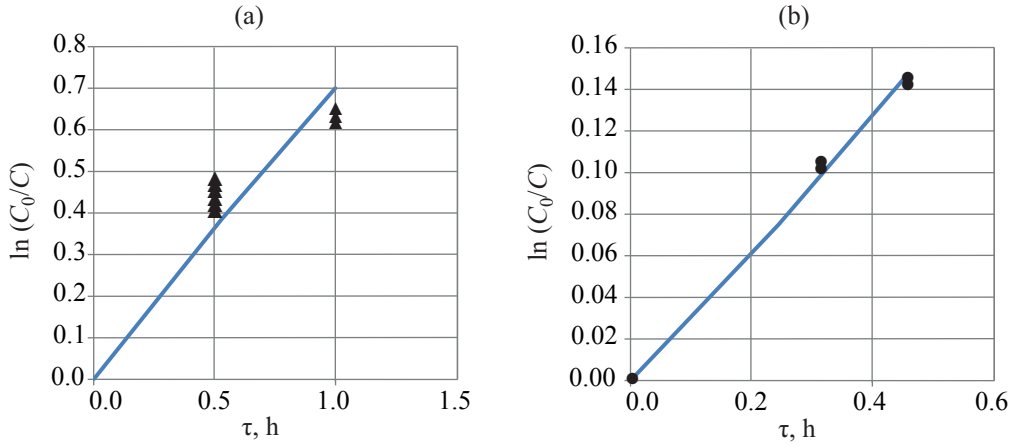

Fig. 3. Linear relationship between the *n*-hexadecane concentration and the conditional contact time for (a) hydrocracking and (b) hydroisomerization reaction.

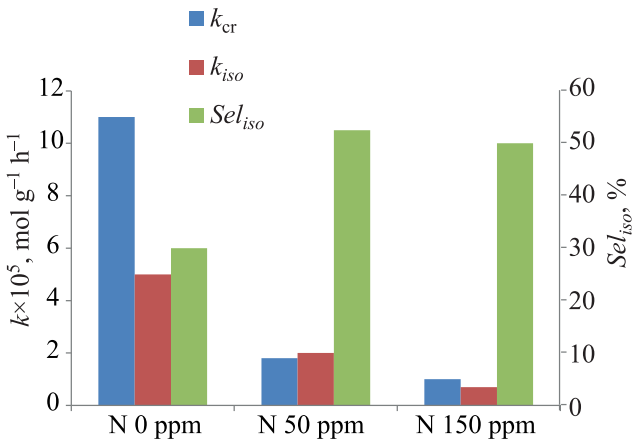

Fig. 4. Selectivity toward hydroisomerization reaction and the rates of hydrocracking and hydroisomerization reactions as functions of the quinoline amount added to the feedstock.

CONCLUSIONS

Bifunctional zeolite-containing transition metal sulfide-based catalysts comprising different zeolite components in varied amounts were synthesized. The resultant materials were examined by low-temperature nitrogen adsorption and NH_3–TPD method, and their catalytic activity for *n*-hexadecane hydroconversion reactions was tested.

In hexadecane hydroconversion on Beta and ZSM-5 zeolite-containing transition metal sulfide-based catalysts the cracking reactions dominated because of a high cracking activity due to a large number of strong acid sites and small zeolite micropores. Reduction in the content of the zeolite component to 5 wt % did not significantly affect the selectivity of the chemical transformations of *n*-hexadecane over the temperature range examined. The use of the bifunctional catalytic compositions based on Beta and ZSM-5 zeolites may be recommended for yielding incremental light components from heavy feedstock processing.

The NH_4NaY zeolite-containing catalyst afforded relatively high (up to 30%) selectivity toward hydroisomerization reaction at moderate cracking activity due to large micropore sizes and moderate acidity of the additive. After further optimization the bifunctional composite catalysts based on NH_4NaY type zeolites and transition metal sulfides will be useful in hydroisomerization and mild hydrocracking of middle distillate fractions aimed at improving their low-temperature properties.

By controlled addition of nitrogen-containing bases to the feedstock the selectivity toward hydroisomerization/hydrocracking reactions can be tuned to some extent via suppressing acid sites of the catalyst. This approach proved effective in our experiments with the sulfide-based bifunctional catalysts. Adding small (50 ppm) amounts of quinoline nitrogen allowed increasing the selectivity toward hydroisomerization reaction from 30 to 60% at a slight decrease of the observed reaction rate.

AUTHOR INFORMATION

N.A. Vinogradov, ORCID: http://orcid.org/0000-0002-7827-7953

M. I. Rubtsova, ORCID: http://orcid.org/0000-0002-3048-8495

A.P. Glotov, ORCID: http://orcid.org/0000-0002-2877-0395

N.V. Tochilin, ORCID: http://orcid.org/0000-0003-3757-9135

V.A. Vinokurov, ORCID: http://orcid.org/0000-0002-0570-6577

A.A. Pimerzin, ORCID: http://orcid.org/0000-0003-1578-5106

ACKNOWLEDGMENTS

We are grateful to Sasol Company (Germany) for providing the pseudoboehmite powder sample.

FUNDING

This study was financially supported by the by the Russian Science Foundation (project no. 19-79-00293).

CONFLICT OF INTEREST

The authors declare no conflict of interest requiring disclosure in this article.

REFERENCES

1. Akhmedov, V.M. and Al-Khowaiter, S.H., *Catal. Rev.*, 2007, vol. 49, no. 1, pp. 33–139. https://doi.org/10.1080/01614940601128427
2. Weyda, H. and Köhler, E., *Catal. Today*, 2003, vol. 81, no. 1, pp. 51–55. https://doi.org/10.1016/S0920-5861(03)00101-9
3. Konnov, S.V., Monakhova, Y.V., Knyazeva, E.E., Yushchenko, V.V., Ponomareva, O.A., and Ivanova, I.I., *Petrol. Chem.*, 2009, vol. 49, no. 1, pp. 79–85. https://doi.org/10.1134/S0965544109010149
4. Grudanova, A.I., Khavkin, V.A., Gulyaeva, L.A., Sergienko, S.A., Krasil'nikova, L.A., and Mis'ko, O.M., *Mir*

Nefteprod., Vestn. Neft. Komp., 2013, vol. 12, pp. 3–7.

5. Onishchenko, M.I. and Maksimov, A.L., *Petrol. Chem*., 2018, vol. 58, no. 8, pp. 651–658. https://doi.org/10.1134/S0965544118080194
6. Lysenko, S.V., Kryukov, I.O., Sarkisov, O.A., Abikenova, A.B., Baranova, S.V., Ostroumova, V.A., Kardashev, S.V., Kulikov, A.B., and Karakhanov, E.A., *Petrol. Chem*., 2011, vol. 51, no. 3, pp. 151–156. https://doi.org/10.1134/S0965544111030091
7. Rezgui, Y. and Guemini, M., *Appl. Catal*., 2005, vol. 282, nos. 1–2, pp. 45–53. https://doi.org/10.1016/j.apcata.2004.11.044
8. Chavarría, J.C., Ramírez, J., González, H., and Baltanas, M.A., *Catal. Today*, 2004, vol. 98, nos. 1–2 spec. issue, pp. 235–242. https://doi.org/10.1016/j.cattod.2004.07.037
9. Guisnet, M., *Catal. Today*, 2013, vols. 218–219, pp. 123–134. https://doi.org/10.1016/j.cattod.2013.04.028
10. Weitkamp, J., Jacobs, P.A., and Martens, J.A., *Appl. Catal*., 1983, vol. 8, no. 1, pp. 123–141. https://doi.org/10.1016/0166-9834(83)80058-X
11. Martens, G.G., Marin, G.B., Martens, J.A., Jacobs, P.A., and Baron, G.V., *J. Catal*., 2000, vol. 195, no. 2, pp. 253–267. https://doi.org/10.1006/jcat.2000.2993
12. Galperin, L.B., *Appl. Catal*., 2001, vol. 209, nos. 1–2, pp. 257–268. https://doi.org/10.1016/S0926-860X(00)00759-6
13. Pimerzin, A.A., Nikul'shin, P.A., Mozhaev, A.V., and Pimerzin, A.A., *Petrol. Chem*., 2013, vol. 53, no. 4, pp. 245–254. https://doi.org/10.1134/S0965544113030067
14. Pimerzin, A.A., Roganov, A.A., Verevkin, S.P., Konnova, M.E., Pilshchikov, V.A., and Pimerzin, A.A., *Catal. Today*, 2019, vol. 329, pp. 71–81. https://doi.org/10.1016/j.cattod.2018.12.034
15. Glotov, A.P., Vutolkina, A.V., Vinogradov, N.A., Pimerzin, A.A., Vinokurov, V.A., and Pimerzin, A.A., *Catal. Today*, 2020, in press. https://doi.org/10.1016/j.cattod.2020.10.010
16. Glotov, A., Stytsenko, V., Artemova, M., Kotelev, M., Ivanov, E., Gushchin, P., and Vinokurov, V., *Catalysts*, 2019, vol. 9, no. 4, pp. 384–396. https://doi.org/10.3390/catal9040384
17. Zhu, S., Liu, S., Zhang, H., Lü, E., and Ren, J., *Cuihua Xuebao/Chin. J. Catal*., 2014, vol. 35, no. 10, pp. 1676–1686. https://doi.org/10.1016/S1872-2067(14)60133-9
18. Smolikov, M.D., Dzhikiya, O.V., Zatolokina, E.V., Kir'yanov, D.I., and Belyi, A.S., *Petrol. Chem*., 2009, vol. 49, no. 6, pp. 473–480. https://doi.org/10.1134/S096554410906005X
19. Yadav, R. and Sakthivel, A., *Appl. Catal. A*, 2014, vol. 481, pp. 143–160. https://doi.org/10.1016/j.apcata.2014.05.010
20. Lian, Z., Yang, C., Shi, L., Meng, X., Liu, N., Yang, Y., and Wang, X., *Appl. Organomet. Chem*., 2018, vol. 32, no. 12, pp. 4587–4598. https://doi.org/10.1002/aoc.4587
21. Meng, X., Lian, Z., Wang, X., Shi, L., and Liu, N., *Fuel*, 2020, vol. 270, pp. 117426–117435. https://doi.org/10.1016/j.fuel.2020.117426
22. Regali, F., Liotta, L.F., Venezia, A.M., Montes, V., Boutonnet, M., and Järås, S., *Catal. Today*, 2014, vol. 223, pp. 87–96. https://doi.org/10.1016/j.cattod.2013.08.028
23. Kinger, G. and Vinek, H., *Appl. Catal. A*, 2001, vol. 218, nos. 1–2, pp. 139–149. https://doi.org/10.1016/S0926-860X(01)00629-9
24. Maesen, T.L.M., Schenk, M., Vlugt, T.J.H., De Jonge, J.P., and Smit, B., *J. Catal*., 1999, vol. 188, no. 2, pp. 403–412. https://doi.org/10.1006/jcat.1999.2673
25. Corma, A., Martinez, A., Pergher, S., Peratello, S., Perego, C., and Bellusi, G., *Appl. Catal. A*, 1997, vol. 152, no. 1, pp. 107–125. https://doi.org/10.1016/S0926-860X(96)00338-9
26. Zhang, W. and Smirniotis, P.G., *J. Catal*., 1999, vol. 182, no. 2, pp. 400–416. https://doi.org/10.1006/jcat.1998.2337
27. Calemma, V., Peratello, S., and Perego, C., *Appl. Catal*., 2000, vol. 190, nos. 1–2, pp. 207–218. https://doi.org/10.1016/S0926-860X(99)00292-6
28. Kazakov, M.O., Nadeina, K.A., Danilova, I.G., Dik, P.P., Klimov, O.V., Pereyma, V.Y., Paukshtis, E.A., Golubev, I.S., Prosvirin, I.P., Gerasimov, E.Y., Dobryakova, I.V., Knyazeva, E.E., Ivanova, I.I., and Noskov, A.S., *Catal. Today*, 2019, vol. 329, pp. 108–115. https://doi.org/10.1016/j.cattod.2019.01.003
29. Kazakov, M.O., Nadeina, K.A., Danilova, I.G., Dik, P.P., Klimov, O.V., Pereyma, V.Y., Gerasimov, E.Y., Dobryakova, I.V., Knyazeva, E.E., Ivanova, I.I., and Noskov, A.S., *Catal. Today*, 2018, vol. 305, pp. 117–125. https://doi.org/10.1016/j.cattod.2017.08.048

30. Lee, S.W. and Ihm, S.K., *Fuel*, 2014, vol. 134, pp. 237–243. https://doi.org/10.1016/j.fuel.2014.05.068
31. Galperin, L.B., *Stud. Surf. Sci. Catal. A*, 2000, vol. 130, pp. 257–262. https://doi.org/10.1016/s0167-2991(00)80966-0
32. Nikulshin, P.A., Ishutenko, D.I., Mozhaev, A.A., Maslakov, K.I., and Pimerzin, A.A., *J. Catal.*, 2014, vol. 312, pp. 152–169. https://doi.org/10.1016/j.jcat.2014.01.014
33. Pimerzin, A.A., Savinov, A.A., Ishutenko, D.I., Verevkin, S.P., and Pimerzin, A.A., *Russ. J. Appl. Chem.*, 2019, vol. 92, no. 12, pp. 1772–1779. https://doi.org/10.1134/S1070427219120198
34. Pimerzin, A., Savinov, A., Vutolkina, A., Makova, A., Glotov, A., Vinokurov, V., and Pimerzin, A., *Catalysts*, 2020, vol. 10, no. 6, p. 594. https://doi.org/10.3390/catal10060594
35. Thommes, M., Kaneko, K., Neimark, A.V., Olivier, J.P., Rodriguez-Reinoso, F., Rouquerol, J., and Sing, K.S.W., *Pure Appl. Chem.*, 2015, vol. 87, nos. 9–10, pp. 1051–1069. https://doi.org/10.1515/pac-2014-1117
36. Lippens, B.C. and de Boer, J.H., *J. Catal.*, 1965, vol. 4, no. 3, pp. 319–323. https://doi.org/10.1016/0021-9517(65)90307-6
37. Dik, P.P., Danilova, I.G., Golubev, I.S., Kazakov, M.O., Nadeina, K.A., Budukva, S.V., Pereyma, V.Y., Klimov, O.V., Prosvirin, I.P., Gerasimov, E.Y., Bok, T.O., Dobryakova, I.V., Knyazeva, E.E., Ivanova, I.I., and Noskov, A.S., *Fuel*, 2019, vol. 237, pp. 178–190. https://doi.org/10.1016/j.fuel.2018.10.012
38. Vu, X.H., Armbruster, U., and Martin, A., *Catalysts*, 2016, vol. 6, no. 12, pp. 183–206. https://doi.org/10.3390/catal6120183
39. Whiting, G.T., Meirer, F., Mertens, M.M., Bons, A.-J., Weiss, B.M., Stevens, P.A., de Smit, E., and Weckhuysen, B.M., *ChemCatChem.*, 2015, vol. 7, no. 8, pp. 1312–1321. https://doi.org/10.1002/cctc.201402897
40. Michels, N.L., Mitchell, S., and Pérez-Ramírez, J., *ACS Catal.*, 2014, vol. 4, no. 8, pp. 2409–2417. https://doi.org/10.1021/cs500353b.
41. Abramova, A.V., Slivinskii, E.V., Goldfarb, Y.Y., Panin, A.A., Kulikova, E.A., and Kliger, G.A., *Kinet. Catal.*, 2005, vol. 46, no. 5, pp. 758–769. https://doi.org/10.1007/s10975-005-0133-5
42. Liao, J., Zhang, Y., Fan, L., Chang, L., and Bao, W., *Ind. Eng. Chem. Res.*, 2019, vol. 58, no. 11, pp. 4572–4580. https://doi.org/10.1021/acs.iecr.8b05046
43. Barzetti, T., Selli, E., Moscotti, D., and Forni, L., *J. Chem. Soc.*, 1996, vol. 92, no. 8, pp. 1401–1407. https://doi.org/10.1039/ft9969201401
44. Alvarez, F., Ribeiro, F.R., Perot, G., Thomazeau, C., and Guisnet, M., *J. Catal.*, 1996, vol. 162, no. 2, pp. 179–189. https://doi.org/10.1006/jcat.1996.0275